ACS OMEGA

Open Access

http://pubs.acs.org/journal/acsodf

Article

A Novel Self-Healing Anticorrosive Inhibitor for Pipeline Corrosion Protection in Geothermal Well Systems

Xiaoguang Jin,* Xiaopeng Yan,* Lei Wang, Song Deng, Linglong Cao, and Jiayun Ma

Cite This: *ACS Omega* 2025, 10, 12088−12096

Read Online

ACCESS | Metrics & More | Article Recommendations

ABSTRACT: The growing demand for energy coupled with the need for environmental sustainability underscores the importance of advancing renewable energy technologies. Among these, geothermal energy stands out as a clean and sustainable resource with substantial potential for heating and power generation. However, the corrosion of materials in geothermal facilities presents a significant operational challenge. This study explores the development of a self-healing anticorrosive coating based on microcapsule technology to address this issue. The proposed coating releases corrosion inhibitors from the microcapsules upon damage, enabling autonomous repair. Microcapsules were fabricated with an oil-soluble imidazoline oleate corrosion inhibitor encapsulated in urea-formaldehyde resin and incorporated into an epoxy resin matrix. The resulting composite coating demonstrated enhanced self-healing properties. Key parameters, including the core-to-wall ratio, healing duration, and microcapsule concentration, were systematically examined for their influence on self-healing efficiency. The performance of the composite was rigorously evaluated through simulated geothermal water corrosion tests under conditions representative of geothermal systems. The results indicate that microcapsules with a core-to-wall ratio of 3:1, using OP-10 as an emulsifier at 0.5 wt % of the core material, exhibited optimal structural integrity and encapsulation efficiency (74.6% core content, 85.7% coating efficiency). Additionally, epoxy resin composites with microcapsule concentrations greater than 20 wt % exhibited effective self-healing of artificially induced damage, demonstrating superior anticorrosive properties crucial for geothermal applications. These findings suggest that the developed self-healing composite holds great potential for mitigating corrosion in geothermal energy systems, contributing to the durability and efficiency of geothermal facilities.

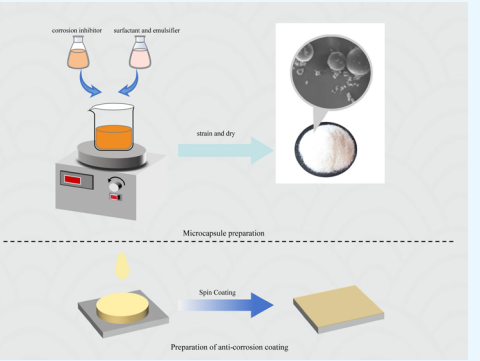

1. INTRODUCTION

With the continuous growth of energy demand and the continuous improvement of environmental protection requirements, strengthening the promotion of clean energy has become an inevitable trend, and geothermal energy, as a renewable clean energy, has great development potential in heating and power generation. However, geothermal facilities have been severely corroded during their use. Because geothermal water contains a variety of corrosive components (O_2, CO_2, HCl, Cl^-, etc.), it can be chemically corroded with metal materials such as geothermal well pipes, and the changing temperature and pressure in geothermal well pipes will also aggravate the corrosion of geothermal well pipes, so the anticorrosion problem of geothermal facilities has also become an urgent problem to be solved, and applying coating is the most economical and convenient anticorrosion means.[1−5]

Coating anticorrosion is a common anticorrosion method in aerospace, engineering construction, automobile manufacturing, petrochemical, and other industries. Traditional anticorrosion coatings mainly perform a physical shielding function to prevent direct contact between external corrosive media and metal substrates. Nowadays, with the demand for long-term service capability and functionality of coatings, smart coatings are gradually becoming a key area of research on anticorrosion coatings. The intelligence of smart coatings is mainly reflected in their ability to respond to changes in environmental factors in a recognizable manner. This response needs to be triggered by an external environment, including specific ions, pH, mechanical damage, temperature, and more. The introduction of intelligent response mechanism into the design of the coating can realize the autonomous response functions such as corrosion resistance, self-repair, self-warning, antibacterial, and wear-resistant according to changes in the external environment, so as to form an active anticorrosion strategy. Hu et al.[6] prepared a Ce-HQ hybrid material by

Received: November 9, 2024
Revised: February 26, 2025
Accepted: March 3, 2025
Published: March 21, 2025

physical blending of cerium nitrate and 8-hydroxyquinoline (8-HQ), and dispersed it into epoxy coatings for corrosion protection of aluminum alloys, endowing epoxy coatings with the ability of corrosion self-healing and fluorescence self-warning. Liu et al.[7] constructed an intelligent anticorrosion system with in situ corrosion sensing and active protection functions: a nanocontainer (ZIF-7@PEG-TA) with ZIF-7 as the core and polyethylene glycol-tannic acid as the shell of the zeolite imidazolate matrix series (ZIFs) was added to the epoxy coating. Li et al. developed a curing agent microcapsule made from poly(methyl methacrylate) and polyetheramine. These epoxy resin microcapsules, along with curing agent microcapsules, were incorporated into a coating. Upon coating damage, both the curing agent and epoxy resin are released simultaneously from the microcapsules, forming a protective layer that repairs the damaged coating. Zhao et al. prepared hollow raspberry-like polystyrene sub-microspheres with perforated surfaces, which contained the corrosion inhibitor BTA (benzotriazole) inside. Under acidic and alkaline conditions, the surface pores of the microcapsules open while they close at a pH of 7. By controlling the release behavior of BTA, these microcapsules, when incorporated into coatings, impart self-healing properties to the coating, effectively enhancing its corrosion resistance. Some scholars have prepared barrier/self-healing dual-function coatings based on single barrier anticorrosion coatings and single self-healing anticorrosion coatings, which can meet different service needs.

Compared with the traditional anticorrosive coatings, the microencapsulated intelligent repair anticorrosive coatings studied in this work can not only realize the physical insulation of the coating and play a passive anticorrosion function but also combine various metal corrosion inhibitors with passive anticorrosion coatings, and when the coating fails, the corrosion inhibitors can be released to continue to play an active anticorrosion function, realize the active self-healing function, and reduce the corrosion rate of the protected metal.[8−10] The dual-function coating combines long-term passive protection with rapid active protection and has superior durability compared to conventional single-function coatings.[11,12] In addition, this work combines the characteristics of the geothermal environment, selects the appropriate microcapsule core, and preferentially selects green organic corrosion inhibitors as remedial measures for the buried coating, which can effectively prevent the pollution of groundwater sources according to environmental protection requirements. As early as 2001, White et al.[13] first proposed a set of microencapsulation self-healing anticorrosive coating material systems, and until now, microcapsule technology is still a research hotspot among scientific researchers.

Microcapsule is a kind of polymer wall envelope or microcontainer, in which a polymer material is used as a microcapsule wall to encapsulate a liquid, solid, or gaseous core material to form tiny solid particles in the form of spheres, usually between 1 and 1000 μm in size. Microencapsulation is this type of micropackaging technology for storing liquids, solids, or gases.[6] The microencapsulated cyst wall is an important factor affecting the microencapsulation process, which usually needs to be nontoxic, with good stability, good film-forming, and nonirritating. There is no reaction between the core material and the capsule wall, there is no miscibility, and the water-soluble core material is selected for the oil-soluble capsule wall material and vice versa. In the self-healing system, polymer materials are the most used, among which urea-formaldehyde resin, melamine formaldehyde resin, and melamine formaldehyde resin are the main ones. Because urea-formaldehyde resin (UF) can be made into high-strength, high-toughness microcapsules and has good antipermeation and wear-resistant properties, UF is currently a research hotspot at home and abroad. Due to the different dosage ratio of microcapsule wall material and core material, the selection of emulsifier will also be different. Because imidazoline corrosion inhibitors have excellent corrosion inhibition performance, good thermal stability, low toxicity, and environmental protection, and are widely used in oil and gas field anticorrosion, and urea-formaldehyde resin is pressure-resistant, wear-resistant, and permeation-resistant, this paper selects imidazoline corrosion inhibitor as the core material and urea-formaldehyde resin as the wall material to prepare microcapsules, designs experiments, studies the influencing factors of microcapsules, gives the conditions for screening the optimal preparation process of corrosion inhibitory dosage microcapsules, and prepares anticorrosive coatings for corrosion inhibitory dosage microcapsules.[14−17]

This study focuses on preparing microcapsules using imidazoline as the core material for its excellent corrosion inhibition, thermal stability, low toxicity, and environmental friendliness, along with urea-formaldehyde resin as the wall material for its pressure resistance and wear resistance. We designed experiments to examine the factors affecting microcapsule formation and establish optimal preparation conditions for corrosion inhibitor-loaded microcapsules. The aim is to develop anticorrosion coatings that are effective in geothermal environments, providing both passive and active protection.

2. EXPERIMENTAL PROCESS

2.1. Experimental Materials and Instruments. Experimental raw materials: oil-soluble imidazoline oleic acid corrosion inhibitor, urea, ammonium chloride, resorcinol, sodium dodecylbenzenesulfonate (SDBS), OP-10, 37% formaldehyde solution, 1% dilute hydrochloric acid, etc.

2.2. Preparation Process.

(1) Dissolve an appropriate amount of emulsifier (OP-10, sodium dodecylbenzenesulfonate (SDBS)) in 250 mL of deionized water at room temperature, stir well to make it completely dissolved;
(2) In the above-mentioned emulsifier solution, add 5 g of urea, 0.5 g of resorcinol, and 0.5 g of ammonium chloride, and mix well to dissolve;
(3) Add the mixture obtained in the first two steps to a 500 mL flask, and adjust the pH value of the reaction system to 3−4 with 1% dilute hydrochloric acid solution;
(4) Slowly add an appropriate amount of the oil-soluble corrosion inhibitor imidazoline oleate and emulsify for 20 min under certain conditions;
(5) After the emulsification is completed, the system is heated to 60 °C in a water bath, and then 12 g of 37% formaldehyde aqueous solution is added, and stirred to room temperature at the specified stirring speed;
(6) After the reaction is completed, the mixture is filtered under vacuum, cleaned with deionized water and ethanol, and dried at 50 °C for 24 h.
(7) First, various contents of imidazoline oleate corrosion inhibitor microcapsules are added to the epoxy resin coating substrate, and isophorone diamine curing agent is added to prepare composite coatings.

https://doi.org/10.1021/acsomega.4c10070
ACS Omega 2025, 10, 12088−12096

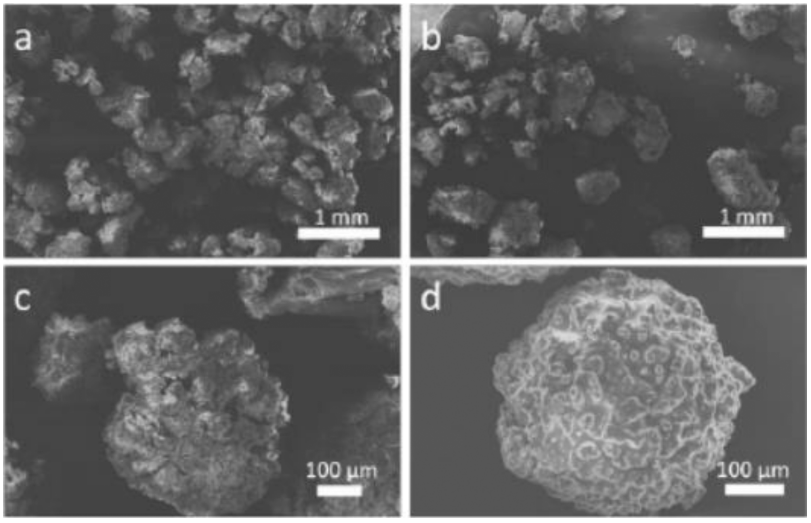

Figure 1. SEM images of microcapsules prepared by ammonium chloride and resorcinol with different content regulators: (a) 0.6:0.4; (b) 0.4:0.6; (c) 0.45:0.45; (d) 0.5:0.5.

2.3. Research on Influencing Factors. *2.3.1. Microcapsule Coating Efficiency.* In this experiment, different microcapsules were prepared using two emulsifiers, sodium dodecylbenzenesulfonate (SDBS) (anionic surfactant) and OP-10 (nonionic surfactant), and the effects of emulsifier type and content, emulsification rate, reaction rate, and core-to-wall ratio on the preparation process of microcapsules were studied. By comparing the core content, coating efficiency, and average particle size of microcapsules and observing them with the help of electron microscopy, the synthesis conditions of microcapsules with excellent performance were finally screened out. Based on this, the coating efficiency is calculated as follows.

First, microcapsules are sampled and ground into a powder. Then, powder was added to 100 mL of absolute ethanol to remove imidazoline oleate (oil-soluble IO), stirred and mixed evenly, and soaked in absolute ethanol for 96 h. During this time, every 24 h, the mixture is allowed to stand, the waste liquid is poured out, and then replaced with new absolute ethanol, and then soaked for 24 h, standing, pouring liquid, changing the liquid, and repeating this process. Finally, the samples were dried for 36 h, and their masses were weighed. The above steps are repeated three times, and the average of the core content and coating efficiency of the microcapsules calculated each time are taken as the final result. The calculation formula is as follows:

$$A = \frac{m_1 - m_2}{m_1}$$

$$B = \frac{m_1 - m_2}{m_3}$$

where:

m_1 indicates the overall mass of the microcapsule;

m_2 indicates the mass of the remaining microcapsule wall material;

m_3 indicates the quality of the core material added during preparation.

2.3.2. Anticorrosion Coating. Artificial scratches were made on the surface of the coating, and the change in Shore hardness of the scratches was continuously measured to evaluate the self-healing ability of microcapsules and epoxy resins.

A conventional epoxy polymeric coating without microcapsules was used as a blank control. After about 40 μm of artificial scratches was made on the surface of each composite coating, the Shore hardness values of the scratch coatings were continuously measured to evaluate and compare their self-healing properties. Then, the results were comprehensively compared to explore the relationship between self-healing ability and the core-to-wall ratio of microcapsules, repair time, and microcapsule content.

After artificially inducing scratches, the Shore hardness of the scratch site was measured with a Shore hardness tester within 0, 1, 2, and 4 h, respectively. This is repeated three times, and the final shore hardness value is determined as the average shore hardness at each time point. Through the variation curve of the Shore hardness value over time, you can intuitively feel the self-healing ability of different composite coatings at room temperature.

2.3.3. Characterization and Analysis of Microcapsules. Scanning electron microscopy (SEM) was used to observe the morphology and particle size of the microcapsules.

3. ANALYSIS OF INFLUENCING FACTORS

3.1. Effect of Regulator Content. Figure 1 illustrates the morphology of microcapsules prepared with varying concentrations of ammonium chloride and resorcinol, as observed by electron microscopy. Ammonium chloride, a strong electrolyte, acts as a crucial regulator by enhancing the ionic strength of the solution. This disrupts the electric double-layer structure of urea-formaldehyde particles, increasing the likelihood of particle collision. Concurrently, resorcinol accelerates the curing process of urea-formaldehyde resins, prevents caking, and enhances the integrity of the core coatings.

In Figure 1a, we observe that when 0.6 g of ammonium chloride and 0.4 g of resorcinol are used, the deposition rate of urea-formaldehyde particles is excessively rapid, preventing proper coating formation. This results in shell agglomeration due to incomplete polymerization. Figure 1b shows that with 0.4 g of ammonium chloride and 0.6 g of resorcinol, a shell forms quickly. However, the rapid curing process does not allow sufficient time for the urea-formaldehyde resin to fully coat the microcapsule core, leading to agglomeration. Figure 1c

https://doi.org/10.1021/acsomega.4c10070
ACS Omega 2025, 10, 12088−12096

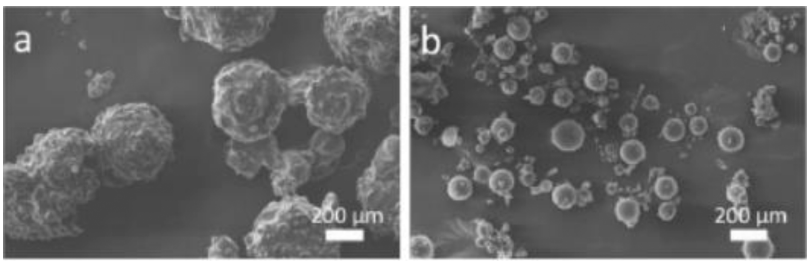

Figure 2. SEM images of microcapsules prepared with different emulsifiers: (a) SDBS, (b) OP-10.

indicates that when 0.45 g each of ammonium chloride and resorcinol is used, the resulting microcapsule shell of the imidazoline oleic acid corrosion inhibitor exhibits incompleteness and surface defects. Finally, Figure 1d demonstrates that with 0.5 g of ammonium chloride and resorcinol each—amounting to 2.5 wt % of the capsule mass—the urea-formaldehyde resin forms and cures at an optimal rate. The resulting microcapsules of the imidazoline oleic acid corrosion inhibitor are uniformly dispersed and show minimal adhesion, highlighting the effectiveness of this formulation.

3.2. The Influence of the Type and Dosage of Emulsifier. In the preparation of microcapsules, selecting an optimal emulsifier is crucial for achieving uniform size and maintaining an intact morphology. Our experiment focused on the comparative effectiveness of two emulsifiers, OP-10 and sodium dodecylbenzenesulfonate (SDBS), in the synthesis of microcapsules. The study revealed that an emulsifier concentration of 0.5 wt % relative to the core material is critical for producing microcapsules with the desired structural integrity. As depicted in Figure 2, the surface morphology of microcapsules containing imidazoline oleate corrosion inhibitors varies significantly with the type of emulsifier used. Microcapsules synthesized with SDBS (referred to as microcapsule a) exhibited several suboptimal characteristics, such as larger particle size, nonuniform distribution, a rough surface texture, and a pronounced tendency toward adhesion and agglomeration. These features contribute to the reduced stability of the microspheres, potentially limiting their applicability in scenarios requiring precision and reliability. Conversely, microcapsules produced using OP-10 as the emulsifier (termed microcapsule b) demonstrated superior qualities, including a smaller and more consistent particle size, smooth surface, and enhanced dispersibility, leading to notably improved stability. These findings suggest that OP-10 is more effective than SDBS in the preparation of microcapsules as it facilitates better control over essential physical properties. Further investigation of the molecular interactions between OP-10 and the core material could provide insights into the mechanisms underlying these improvements. Additionally, exploring the performance of these microcapsules in various environmental conditions would be beneficial to assessing their potential for real-world applications, particularly where stability and uniformity are paramount.

3.3. Effect of Rotational Speed during Emulsification. Table 1 shows the values of three parameters for different microcapsules prepared using OP-10 as an emulsifier at different emulsification rates, and it can be seen that the average particle size, core content, and coating efficiency of microcapsules gradually increase with the decrease of emulsification rate. As shown in Table 1, the coating efficiency of microcapsules prepared at an emulsion rate of 1100 rpm is the highest. Figure 3 is the SEM image of various microcapsules, and it can be seen that the dispersion of the microcapsules gradually increases as the emulsification rate increases. According to the chart data, compared with the core content and coating efficiency, the particle size of microcapsules is greatly affected by the emulsification rate.

Table 1. Parameters of Microcapsules Prepared at Different Emulsification Rates

numbering	emulsifiers	emulsification speed (rpm)	average particle size (μm)	capsule core content (%)	coating efficiency (%)
a	OP-10	900	170	63.5	62.9
b	OP-10	1000	155	65.2	64.3
c	OP-10	1100	132	67.1	65.2

3.4. Effect of Rotational Speed during Reaction. Table 2 shows the values of three parameters for microcapsules prepared with OP-10 as the emulsifier at different reaction rates. The data showed that the particle size of the microcapsules gradually decreased with the increase of the reaction rate, while the core content and coating efficiency of the capsules increased first and then decreased. As can be seen from the table, the coating efficiency is highest at 700 rpm. This indicates that the overall efficiency of the microcapsules prepared at 700 rpm is good. Figure 3 shows SEM images of various microcapsules with a gradual increase in reaction rate and easier dispersion between particles of microcapsules. This may be because the raw materials used to prepare the microcapsules do not react sufficiently when the reaction rate is small, forming some impurities that do not contribute to the formation of the microcapsules, which will weaken the bond between the surface of the microcapsules and the epoxy resin substrate. Therefore, microcapsules prepared with the emulsifier OP-10 and a reaction rate of 700 rpm were found to be the best, and the coating efficiency was the highest.

According to the above test data, the reaction speed of the system has a great influence on the average particle size, core material content, and coating efficiency of microcapsules. It can be seen that the reaction speed is a crucial factor in the preparation of microcapsules.

3.5. Effect of Core-to-Wall Ratio (IO:UF). The ratio of core material to wall material is the key factor affecting the core coating during the microencapsulation process of the corrosion inhibitor. The more wall material content is used, the thicker the microcapsule wall film will be, and conversely, if there is too little wall material, then the coverage of the core material will be poor. Table 3 shows the values of each parameter for microcapsules made with emulsifier OP-10 at different core-to-wall ratios. When the core-to-wall ratio (IO:UF) gradually decreases, the size of the prepared microcapsules decreases,

https://doi.org/10.1021/acsomega.4c10070
ACS Omega 2025, 10, 12088−12096

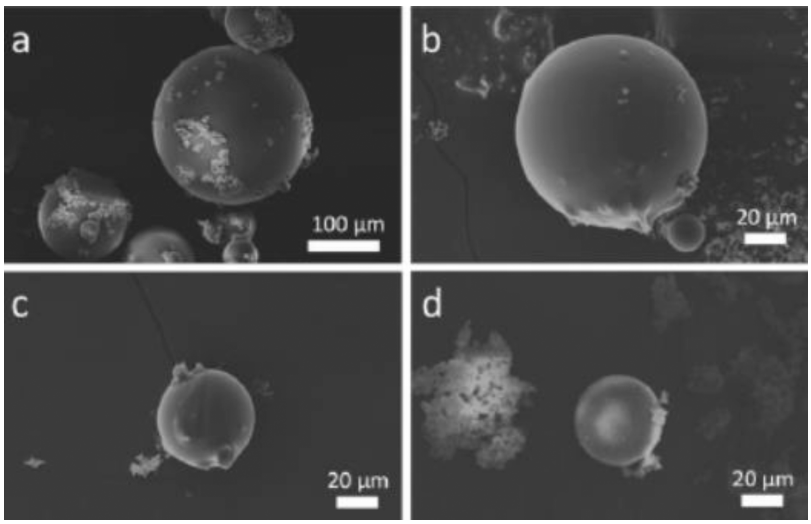

Figure 3. SEM images of microcapsules prepared at different reaction rates: (a) 600; (b) 650; (c) 700; (d) 750.

Table 2. Parameters of Microcapsules Prepared at Different Reaction Rates

numbering	emulsifiers	emulsification rate (rpm)	average particle size (μm)	capsule core content (%)	coating efficiency (%)
a	OP-10	600	130	69.7	69.2
b	OP-10	650	85	72.8	82.5
c	OP-10	700	64	73.7	84.8
d	OP-10	750	50	71.3	78.7

Table 3. Parameters of Microcapsules Prepared under Different Core-to-Wall Ratios

numbering	emulsifiers	core-to-wall ratio	average particle size (μm)	capsule core content (%)	coating efficiency (%)
a	OP-10	3:1	324	74.6	85.7
b	OP-10	2:1	286	60.5	78.5
c	OP-10	1:1	235	52.1	60.9

and the coating efficiency and core material content decrease. Figure 3 shows the cross-sectional SEM images of different microcapsules, and it can be seen that when the core-to-wall ratio is 1:1, the microcapsule wall is the thickest, and the larger the core-to-wall ratio, the thinner the capsule wall, the average particle size of the microcapsule decreases, and the core material content of the microcapsule is also reduced. Therefore, microcapsules with different wall thicknesses can be prepared by adjusting the proportion of core material and wall material according to actual needs. Theoretically, the microcapsule coating with a core-to-wall ratio of 3:1 has the largest core material content, the highest coating efficiency, and better self-healing performance.

Combined with the above analysis, the core-to-wall ratio and the system reaction rate are the two most critical factors in the preparation of microcapsules, and the particle size, core material content, and coating efficiency of microcapsules can be adjusted and controlled by controlling these two factors, so as to synthesize imidazoline oleate corrosion inhibitor microcapsules with excellent performance. In addition, it can be concluded that the characteristic parameters of microcapsules are affected by the emulsification rate but not by comparison. Finally, through the systematic analysis of the preparation process of imidazoline oleate corrosion inhibitor microcapsules, it was found that microcapsules with excellent performance could be prepared by satisfying the following conditions: the core-to-wall ratio (IO:UF) was 3:1, 0.5 g of regulators ammonium chloride and resorcinone were added, and OP-10 was selected as the emulsifier, the dosage was 0.5 wt % of the core content, the emulsification rate was 1200 r/min, and the reaction rate was 700 r/min. Microcapsules are prepared by a one-step in situ polymerization method with regular morphology and the highest encapsulation efficiency.

3.6. Effect of Core-to-Wall Ratio of Microcapsules on the Self-Healing Properties of Coatings. Table 4 records

Table 4. Shore Hardness Values of Composite Coatings with Different Core-to-Wall Ratios at Room Temperature after Artificial Scratches

time	shore hardness values of microcapsules and epoxy resin composite coatings at different core-to-wall ratios		
	3:1	2:1	1:1
0	92	91	91
1	78	82	80
2	87	84	83
3	90	87	85
4	92	89	90

the presence of 20 wt % microcapsules at room temperature (25 °C) with core-to-wall ratios of 3:1, 2:1, and 1:1, respectively. Figure 4.2 shows the corresponding change curve of the variation of the Shore hardness value during the self-healing process of the composite coating after artificial scratches. According to Figure 4, when the microcapsule content is 20 wt % and the core-to-wall ratio of the microcapsule is 3:1, the composite coating of microcapsule and epoxy resin has the best self-ability. The Shore hardness of each composite coating before scratching is between 90 and 92, and after being artificially scratched, the Shore hardness will first decrease rapidly and then slowly recover to between 88 and 92 within 1−4 h, indicating that the 22 layers of composite coating have self-healing ability. When the core-to-wall ratio decreases (i.e., the proportion of urea-containing formaldehyde resin in the capsule wall increases), the viscosity

https://doi.org/10.1021/acsomega.4c10070
ACS Omega 2025, 10, 12088−12096

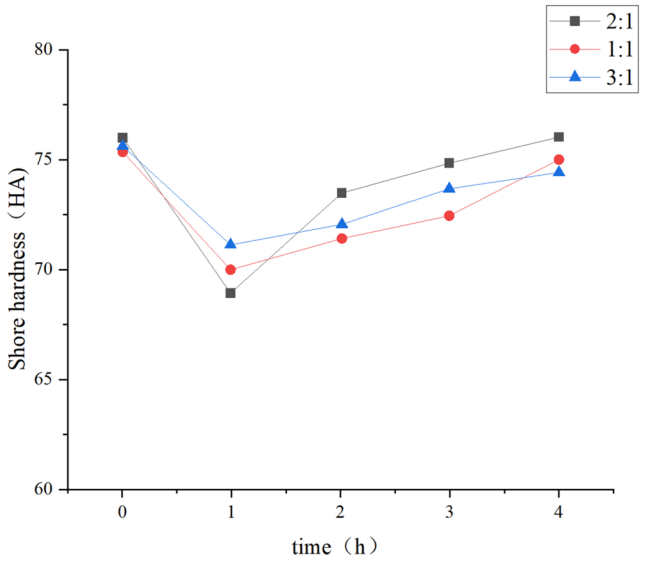

Figure 4. Shore hardness curves of composite coatings with different core-to-wall ratios at room temperature after artificial scratches.

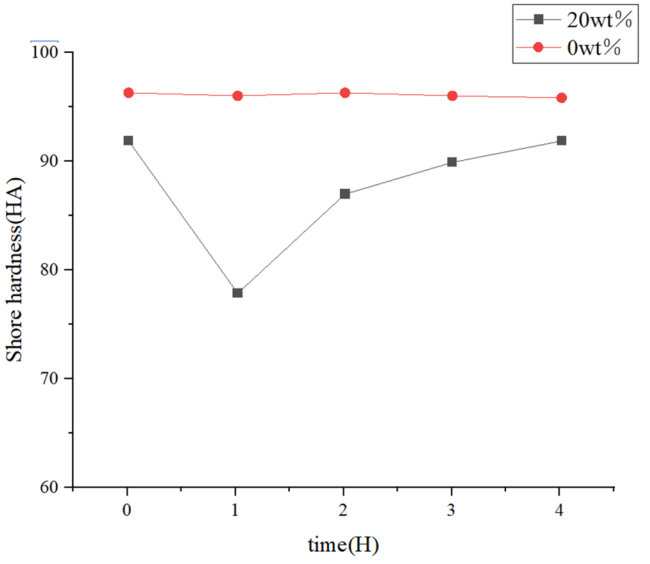

Figure 5. Shore hardness curves of blank coating and composite coating after artificial scratching at room temperature.

of the corrosion inhibitor in the microcapsule decreases and the fluidity increases. Therefore, when there is damage such as microcracks on the surface of the coating, the imidazoline oleate corrosion inhibitor can be evenly distributed at the cracks and the corrosion inhibitor continues to play a role to help repair the cracks in the coating. Therefore, the core-to-wall ratio of microcapsules is a key factor affecting the self-healing properties of the microcapsule composite coatings.

3.7. Effect of Time on the Self-Healing Properties of Coatings. Table 5 shows the variation of Shore hardness values at room temperature (25 °C) for an epoxy composite coating (core/wall ratio of 3:1) containing 20 wt % microcapsules at different times during the self-healing process after manual scraping. As shown in Figure 5, the fully cured conventional epoxy coating has no significant change in Shore hardness values, ranging from 95.5 to 96.5 and containing 20 wt %. The Shore hardness value of the microencapsulated epoxy composite coating first dropped to 76.2 and then rose to 91.7. Other things being equal, the time in the repair process has a certain effect on the self-healing performance of the corrosion inhibitor microcapsule and epoxy resin composite coatings.

Table 5. Shore Hardness Values Blank and Composite Coatings after Artificial Scratches at Room Temperature

	shore hardness values for blank coatings and composite coatings	
time	0 wt %	20 wt %
0	96.5	92
1	96	78
2	96.2	87
3	96.15	90
4	96	92

3.8. Effect of Microcapsule Content on the Self-Healing Properties of Coatings. Figure 6 shows the OM plots of microcapsules with different microcapsule contents (3:1 core-to-wall ratio) and epoxy resin composite coating at room temperature (25 °C) under an optical microscope after 4 h of artificial scratching. As can be seen from Figure 6, the composite coating is able to achieve complete repair of artificially manufactured scratches at microcapsule levels of 20 wt % or higher, suggesting that all other things being equal, the more microcapsules in the composite coating, the stronger the self-healing ability of the composite coating, but Figure 6 shows that the higher the microcapsule content, the lower the Shore hardness value after fracture of the composite coating. In general, when the microcapsule content is 20 wt %, the comprehensive characteristics of the composite coating are better, which has both self-healing characteristics and certain strength. Therefore, the microencapsulation content is an important factor in the self-healing properties of composite coatings.

4. CORROSION SIMULATION EXPERIMENTS TO EXPLORE THE ANTICORROSION CHARACTERISTICS OF ANTICORROSION COATINGS

4.1. Geothermal Water Corrosion Simulation Experiment. According to the optimal process conditions for the preparation of microcapsules, the microcapsules of imidazoline oleate corrosion inhibitor were synthesized, and the microcapsules without microcapsules and the content of 20 wt % were embedded in the coating substrate, and the ordinary epoxy resin coating and microcapsule/epoxy resin composite coating were made after curing by isophorone diamine curing agent.[18−21] Then, a corrosion simulation test bench was established, and the main chemical compositions were CO_2, H_2S, Ca^{2+}, Mg^{2+}, Cl, and HCO^{3-} by simulating the corrosion solution. To use analytical reagents, the corrosion simulation solution must be at a temperature of 75 °C with a pH between 3 and 4. The carbon steel rods are first sanded with sandpaper with a grit size of 80 to 600 and then cleaned with alkali and ethanol. To prevent the formation of an oxide layer on the surface of the steel substrate, it is air-dried under compressed air and allowed at 60 °C for 15 min, after which it is immediately coated. Prior to the test, two coated steel rods should be placed on a stainless steel tray in an autoclave and 3 L of simulation fluid should be injected to fully immerse the

https://doi.org/10.1021/acsomega.4c10070
ACS Omega 2025, 10, 12088−12096

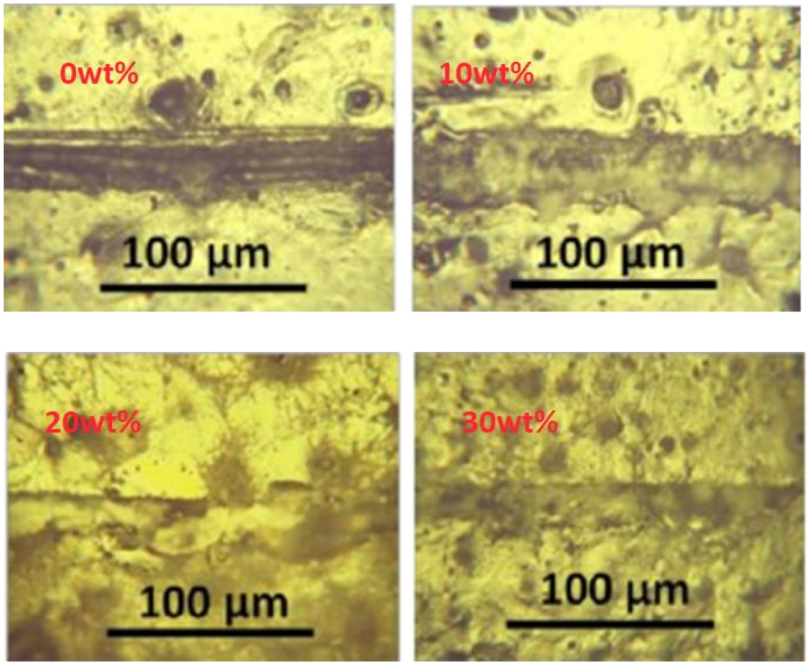

Figure 6. OM plot of composite coatings with different microcapsule contents at room temperature after 4 h of human scratching.

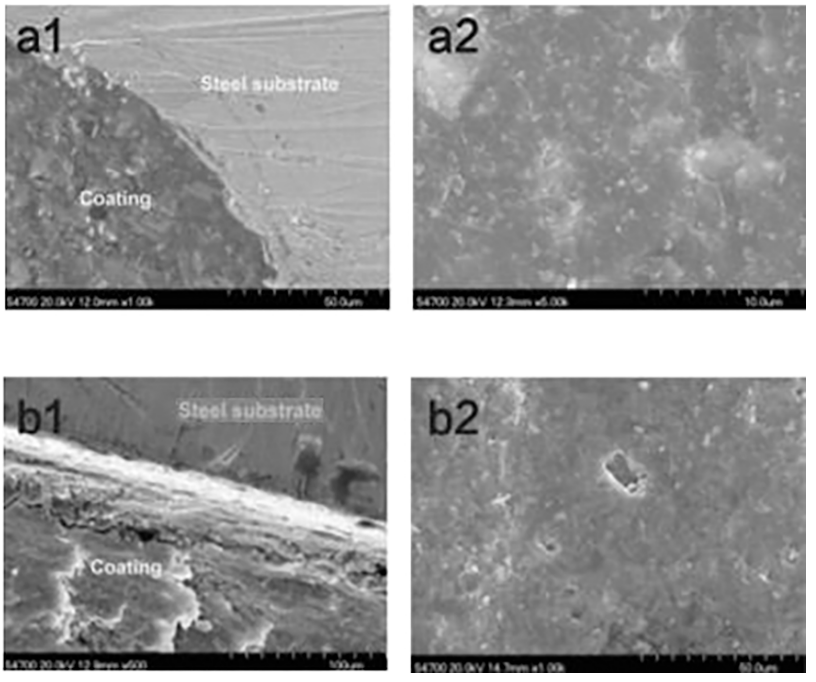

Figure 7. SEM diagram of coating section and surface topography after corrosion simulation test: (a1) impermeability; (a2) noncorroded; (b1) crack; (b2) pinhole.

carbon steel rods.[22−25] The rods are then bubbled with high-purity nitrogen for 2 h to remove dissolved oxygen. At the end of the 31-day corrosion test, the temperature in the autoclave is reduced to room temperature, and the pressure is restored to atmospheric pressure. Subsequently, the test rods were washed with double-distilled water and dried in an oven at 50 °C.[26−29]

4.2. Morphological Characteristics of the Coating before and after the Corrosion Simulation Test. The morphological characteristics of the surface and section of the coating were analyzed by SEM, and the surface and section morphological characteristics of the coating after the geothermal water corrosion simulation test are shown in Figure 7, in which panels a1 and a2 are microcapsules containing 20 wt % after the test, respectively/epoxy resin composite coating section and surface morphology, and panels b1 and b2 are the section and surface morphology of ordinary epoxy resin coating without microcapsules after the test, respectively.

(1) As can be seen from Figure 7a1, the contact between the section of the corrosion inhibitor/epoxy resin composite coating and the carbon steel substrate is very tight and has not yet been penetrated by corrosive media. In Figure 7a2, no obvious corrosion holes or corrosion

https://doi.org/10.1021/acsomega.4c10070
ACS Omega 2025, 10, 12088−12096

channels were found on the surface of the composite coating, indicating that the corrosion inhibitor microcapsules in the composite coating improved the corrosion resistance of the anticorrosion coating, or that the corrosion inhibitor microcapsules were repaired independently after the coating was damaged.

(2) Figure 7b1 shows that the contact surface of the epoxy coating without microcapsules and the substrate is cracked as adhesion decreases. In Figure 7b2, small holes of about 5 μm appear on the surface of the coating, which roughens the surface of the coating, through which the medium penetrates into the inside of the coating, thereby reducing its protective effect. In general, the addition of imidazoline oleate corrosion inhibitor microcapsules to the epoxy resin coating can realize the self-improvement of the composite coating's restorative effect.

5. RESULTS AND DISCUSSION

In this study, oil-soluble imidazoline oleate corrosion inhibitor microcapsules coated with urea-formaldehyde resin were designed and synthesized. These microcapsules were incorporated into an epoxy resin matrix to produce an epoxy composite coating containing corrosion inhibitor microcapsules. The self-healing properties of the composite coatings were first qualitatively assessed through artificial scratching experiments, followed by an analysis of the influencing factors. Specifically, the effects of the core-to-wall ratio, repair time, and microcapsule content on the self-healing performance were investigated. Subsequently, the self-healing efficacy of the microcapsules and epoxy composite coatings was validated through indoor geothermal water corrosion simulation tests. The following conclusions were drawn from the study:

(1) The synthesis process for the oil-soluble imidazoline oleate corrosion inhibitor microcapsules was optimized. The optimal conditions for preparing microcapsules involved a core-to-wall ratio of 3:1 (urea-formaldehyde resin to imidazoline oleate), with 2.5 wt % of resorcinol and ammonium chloride as regulating agents and 0.5 wt % OP-10 as the emulsifier. The emulsification speed was set to 1200 rpm, and the reaction speed was 700 rpm. Under these conditions, the microcapsules exhibited a well-preserved morphology with a core content of 74.6% and a coating efficiency of 85.7%. These results indicate that the developed microcapsules possess high structural integrity and encapsulation efficiency, making them suitable for incorporation into corrosion-resistant coatings.

(2) Investigation of the self-healing properties of oil-soluble imidazoline oleic acid corrosion inhibitor microcapsules and epoxy resin composites in artificial scratch tests: The test results show that the main factors affecting the self-healing properties of microcapsules and epoxy resin composites are core-to-wall ratio, microcapsule content, and repair time. When the ratio of the oil-soluble corrosion inhibitor imidazoline oleate microcapsules to the core wall is 3:1 and the content of the microcapsules is more than 20 wt %, the epoxy resin composites can achieve self-healing after manual scraping, indicating that their self-healing performance is good.

(3) Study on the self-healing performance of oil-soluble imidazoline corrosion inhibitor microcapsules and epoxy resin composite materials in a geothermal well corrosion simulation environment: The results from geothermal water corrosion simulation experiments on microcapsule-epoxy resin composite systems demonstrate the effectiveness of the composite coating in mitigating corrosion. In the experimental setup, carbon steel rods coated with the epoxy resin composite were compared with a control group using epoxy resin without microcapsules. After 31 days of exposure to simulated geothermal water at 75 °C, the composite coating exhibited excellent adhesion between the coating and the substrate, with no visible etching or degradation at the interface. The coating surface remained smooth, and no significant damage was observed, indicating that the composite coating maintained its anticorrosive properties and demonstrated self-healing capabilities in the geothermal environment. These findings suggest that the microcapsule-embedded epoxy resin composite is effective in both preventing corrosion and facilitating self-repair.

AUTHOR INFORMATION

Corresponding Authors

Xiaoguang Jin − *Sinopec Key Laboratory of Geothermal Resources Exploitation and Utilization, Beijing 100000, China*; Email: jinxg82549.sripe@sinopec.com

Xiaopeng Yan − *Sinopec Key Laboratory of Geothermal Resources Exploitation and Utilization, Beijing 100000, China; School of Petroleum Engineering and natural gas, Changzhou University, Changzhou 213164, China; CNPC-CZU Innovation Alliance, Changzhou University, Changzhou 213164, China*; orcid.org/0000-0002-7422-2963; Email: lcm_yxp2017@126.com

Authors

Lei Wang − *Sinopec Key Laboratory of Geothermal Resources Exploitation and Utilization, Beijing 100000, China*

Song Deng − *School of Petroleum Engineering and natural gas, Changzhou University, Changzhou 213164, China*; orcid.org/0000-0003-4322-8534

Linglong Cao − *School of Petroleum Engineering and natural gas, Changzhou University, Changzhou 213164, China*

Jiayun Ma − *School of Petroleum Engineering and natural gas, Changzhou University, Changzhou 213164, China*

Complete contact information is available at: https://pubs.acs.org/10.1021/acsomega.4c10070

Notes

The authors declare no competing financial interest.

ACKNOWLEDGMENTS

This research was supported by the open fund of Sinopec Key Laboratory of Geothermal Resources Exploitation and Utilization (36650000-23-ZC0607-0053), the Natural Science Foundation of Jiangsu Province (BK20240970), and 2023 Science and Technology Innovation Talent Project of CNPC-CZU Innovation Alliance (CCIA 2023-10). The authors express their sincere gratitude to all participants for their valuable contributions.

REFERENCES

(1) Madirisha, M.; Hack, R.; Meer, F. D. V. D. Simulated microbial corrosion in oil, gas and non-volcanic geothermal energy installations: The role of biofilm on pipeline corrosion. *Energy Rep.* **2022**, *8*, 2964−2975.

(2) Wang, G. G.; Zhu, L. Q.; Liu, H. C.; et al. Galvanic corrosion of Ni−Cu−Al composite coating and its anti-fouling property for metal pipeline in simulated geothermal water. *Surf. Coat. Technol.* **2012**, *206* (18), 3728−3732.

(3) Kang, Ruirui.; Fang, Daqing.; Chen, Cai. yang.et al. Coatings & Coatings. 2024; Vol. *54* 1, pp 66−73.

(4) Ye, Y.; Zhang, D.; Liu, T.; et al. Superior corrosion resistance and self-healable epoxy coating pigmented with silanzied trianiline-intercalated graphene. *Carbon* **2019**, *142*, 164−176.

(5) Yang, S. H.; Huang, Y. X.; Li, P. S.; et al. Tannin-based modified graphene oxide anti-corrosion composite coating with favourable corrosion inhibition,self-healing and photothermal conversion properties. *Corros. Sci.* **2024**, *231*, No. 111956.

(6) Hu, Y.; Cao, X.; Ma, X.; et al. A bifunctional epoxy coating doped by cerium (III)-8-hydroxyquinoline: Early self-reporting and stimuli-responsive inhibition on corrosion of Al substrate. *Prog. Org. Coat.* **2023**, *182*, No. 107616.

(7) Liu, C.; Qian, B.; Hou, P.; et al. Stimulus Responsive Zeolitic Imidazolate Framework to Achieve Corrosion Sensing and Active Protecting in Polymeric Coatings. *ACS Appl. Mater. Interfaces* **2021**, *13* (3), 4429−4441.

(8) Manabe, K.; Norikane, Y. Graphene composite self-healing antifog/frost-resist transparent coatings with zwitter wettability. *Surf. Interfaces* **2023**, *42*, No. 103363.

(9) Zhao, G.; Li, J.; Ren, X.; et al. Few-layered graphene oxide nanosheets as superior sorbents for heavy metal ion pollution management. *Environ. Sci. Technol.* **2011**, *45* (24), 10454−10462.

(10) Kasaeian, M.; Ghasemi, E.; Ramezanzadeh, B.; et al. Construction of a highly effective self-repair corrosion resistant epoxy composite through impregnation of 1Hbenzimidazole corrosion inhibitor modified graphene oxide nanosheets(GO-BIM). *Corros. Sci.* **2018**, *145*, 119−134.

(11) Zhong, F.; He, Y.; Wang, P. Q.; et al. Novel pH-responsive self-healing anti-corrosion coating with high barrier and corrosion inhibitor loading based on reduced graphene oxide loaded zeolite imidazole framework. *Colloids Surf., A* **2022**, *642*, No. 128641.

(12) Ding, R.; Chen, S.; Zhou, N.; et al. The diffusion-dynamical and electrochemical effect mechanism of oriented magnetic graphene on zinc-rich coatings and the electrodynamics and quantum mechanics mechanism of electron conduction in graphene zinc-rich coatings. *J. Alloys Compd.* **2019**, *784*, 756−768.

(13) White, S. R.; Sottos, N. R.; Geubelle, P. H.; et al. Autonomic healing of polymer composites. *Nature* **2001**, *409* (6822), No. 794.

(14) Shi, Y.; Li, Z.; Li, Z. Synthesis and evaluation of scale inhibitor with high-temperature resistance and low corrosion capability for geothermal exploitation. *J. Pet. Sci. Eng.* **2022**, *218*, No. 110976.

(15) Kobbekaduwa, Dhanushka.; et al. Effect of organic corrosion inhibitors on the behaviour of repair mortars and reinforcement corrosion. *Constr. Build. Mater.* **2024**, *451*, No. 138787.

(16) Wei, K.; Zhao, X.; Zhang, Z.; Yuan, Y.; Kong, W.; Zhang, Y. Duplex Coating Combing Vanadate-Intercalated Layered Double Hydroxide and Ce-Doped Sol−Gel Layers on Aluminum Alloy for Active Corrosion Protection. *Materials* **2023**, *16*, No. 775.

(17) Chen, Z.; Scharnagl, N.; Zheludkevich, M. L. Micro/nanocontainer-based intelligent coatings: Synthesis, performance and applications-A review. *Chemical Engineering Journal*. 2022.

(18) Chen, Y.; Wu, L.; Yao, W.; et al. "Smart" micro/nano container-based self-healing coatings on magnesium alloys:a review. *J. Magnesium Alloys* **2023**, *11* (7), 2230−2259.

(19) Wang, J.; Tan, W.; Yang, H.; et al. Towards weathering and corrosion resistant,self-warning and self-healing epoxy coatings with tannic acid loaded nanocontainers. *npj Mater. Degrad.* **2023**, *7* (1), No. 12.

(20) Sun, C.; Liu, C.; Wang, Y.; et al. Corrosion sensing and self-healing composite coatings on magnesium alloy AZ31 enabled by stimuli-responsive microcapsules loaded with phenolphthalein and epoxy resin. *Prog. Org. Coat.* **2024**, *186*, No. 108043.

(21) Li, W.; Tao, J.; Chen, Y.; et al. Porous microspheres with corrosion sensing and active protecting abilities towards intelligent self-reporting and anti-corrosion coating. *Prog. Org. Coat.* **2023**, *178*, No. 107468.

(22) Liu, J.; Huang, W.; Zhang, K.; et al. Early warning and self-repair properties of o-phenanthroline modified graphene oxide anti-corrosion coating. *Prog. Org. Coat.* **2024**, *189*, No. 108274.

(23) Wei, K.; Wei, Y.; Zhang, Y.; et al. In situ synthesis of ZIF-8 loaded with 8-hydroxyquinoline composite via a host-guest nano-confinement strategy for high-performance corrosion protection. *Corros. Sci.* **2024**, *227*, No. 111731.

(24) Wang, J. P.; Wang, J. K.; Zhou, Q.; et al. Adaptive polymeric coatings with self-reporting and self-healing dual functions from porous core-shell nanostructures. *Macromol. Mater. Eng.* **2018**, *303* (4), No. 1700616.

(25) Liu, T.; Zhang, D.; Ma, L.; et al. Smart protective coatings with self-sensing and active corrosion protection dual functionality from pH-sensitive calcium carbonate microcon tainers. *Corros. Sci.* **2022**, *200*, No. 110254.

(26) Zhao, D.; Wang, M.; Xu, Y.; et al. The Fabrication and Corrosion Resistance of Benzotriazole-loaded Raspberry-like Hollow Polymeric Microspheres. *Surf. Coat. Technol.* **2014**, *238*, 15−26.

(27) Li, Q.; Mishra, A. K.; Kim, N. H.; et al. Effects of Processing Conditions of Poly(Methylmethacrylate) Encapsulated Liquid Curing Agent on the Properties of Self-healing Composites. *Composites, Part B* **2013**, *49*, 6−15.

(28) Wang, T.; Tan, L. H.; Ding, C.; et al. Redox-triggered Controlled Release Systems-based Bi-layered Nanocomposite Coating with Synergistic Self-healing Property. *J. Mater. Chem. A* **2017**, *5* (4), 1756−1758.

(29) Carneiro, J.; Tedim, J.; Fernandes, S.; et al. Chitosan-based Self-healing Protective Coatings Doped with Cerium Nitrate for Corrosion Protection of Aluminum Alloy 2024. *Prog. Org. Coat.* **2012**, *75* (1−2), 8−13.

https://doi.org/10.1021/acsomega.4c10070
ACS Omega 2025, 10, 12088−12096